

Journal Pre-proof

miR-129-5p: A key factor and therapeutic target in amyotrophic lateral sclerosis

Alessia Loffreda, Monica Nizzardo, Alessandro Arosio, Marc-David Ruepp, Raffaele A. Calogero, Stefano Volinia, Marco Galasso, Caterina Bendotti, Carlo Ferrarese, Christian Lunetta, Mafalda Rizzuti, Antonella Ronchi, Oliver Mühlemann, Lucio Tremolizzo, Stefania Corti, Silvia M.L. Barabino



PII: S0301-0082(20)30058-7

DOI: <https://doi.org/10.1016/j.pneurobio.2020.101803>

Reference: PRONEU 101803

To appear in: *Progress in Neurobiology*

Received Date: 23 June 2019

Revised Date: 2 April 2020

Accepted Date: 9 April 2020

Please cite this article as: Loffreda A, Nizzardo M, Arosio A, Ruepp M-David, Calogero RA, Volinia S, Galasso M, Bendotti C, Ferrarese C, Lunetta C, Rizzuti M, Ronchi A, Mühlemann O, Tremolizzo L, Corti S, Barabino SML, miR-129-5p: A key factor and therapeutic target in amyotrophic lateral sclerosis, *Progress in Neurobiology* (2020), doi: <https://doi.org/10.1016/j.pneurobio.2020.101803>

This is a PDF file of an article that has undergone enhancements after acceptance, such as the addition of a cover page and metadata, and formatting for readability, but it is not yet the definitive version of record. This version will undergo additional copyediting, typesetting and review before it is published in its final form, but we are providing this version to give early visibility of the article. Please note that, during the production process, errors may be discovered which could affect the content, and all legal disclaimers that apply to the journal pertain.

© 2020 Published by Elsevier.

miR-129-5-p: a key factor and therapeutic target in amyotrophic lateral sclerosis

Alessia Loffreda^{1#}, Monica Nizzardo^{2,3}, Alessandro Arosio⁴, Marc-David Ruepp^{5*}, Raffaele A. Calogero⁶, Stefano Volinia⁷, Marco Galasso⁷, Caterina Bendotti⁸, Carlo Ferrarese^{4,9}, Christian Lunetta¹⁰, Mafalda Rizzuti³, Antonella Ronchi¹, Oliver Mühlemann⁵, Lucio Tremolizzo^{4,9}, Stefania Corti^{2,3§}, Silvia ML Barabino^{1§}

¹ Department of Biotechnology and Biosciences, University of Milano-Bicocca, Milan, Italy

² Dino Ferrari Centre, Neuroscience Section, Department of Pathophysiology and Transplantation (DEPT), University of Milan

³ Foundation IRCCS Ca' Granda Ospedale Maggiore Policlinico, Neurology Unit, Milan, Italy.

⁴ School of Medicine and Surgery and Milan Center for Neuroscience (NeuroMI), University of Milano-Bicocca, 20052 Monza, (MB), Italy

⁵ Department of Chemistry and Biochemistry, University of Bern, 3012 Bern, Switzerland

⁶ Department of Molecular Biotechnology and Health Sciences, University of Torino, 10126 Turin, Italy

⁷ Department of Morphology, Surgery and Experimental Medicine, Università degli Studi, 44121 Ferrara, Italy

⁸ Department of Neuroscience, IRCCS-Istituto di Ricerche Farmacologiche "Mario Negri", 20156 Milan, Italy

⁹ Neurology Unit, San Gerardo Hospital, Monza, (MB), Italy

¹⁰ NeuroMuscular Omnicentre (NEMO), Fondazione Serena Onlus, 20162 Milan, Italy

#Present address: Istituto Scientifico Ospedale San Raffaele, Centro di Imaging Sperimentale 20132 Milano, Italy.

*Present address: UK Dementia Research Institute at King's College London, Institute of Psychiatry, Psychology and Neuroscience, King's College London SE5 9NU London, UK

Running Title: miRNA expression in ALS

§Corresponding authors:

Silvia M.L. Barabino

Department of Biotechnology and Biosciences

University of Milano-Bicocca, Piazza della Scienza, 2

I-20126 Milano, Italy

Phone: +39-02-6448 3352

Stefania Corti

Dino Ferrari Centre, Neuroscience Section,

Department of Pathophysiology and Transplantation (DEPT), University of Milan, Neurology Unit, IRCCS Foundation Ca' Granda Ospedale Maggiore Policlinico, Milan, Italy.

Phone: +39-02-55055817

Highlights

- The abundance of components in the miRNA processing machinery is altered in a SOD1-linked cellular model
- miR-129-5p was increased in different models of SOD1-linked ALS and in peripheral blood cells of sporadic ALS patients.
- We demonstrated that miR-129-5p upregulation causes the downregulation of one of its targets: the RNA-binding protein ELAVL4/HuD.
- Overexpression of pre-miR-129-1 inhibited neurite outgrowth and differentiation via HuD silencing *in vitro*, while its inhibition with an antagomir rescued the phenotype.
- Administration of an antisense oligonucleotide (ASO) inhibitor of miR-129-5p to an ALS animal model, SOD1(G93A) mice, result in a significant increase in survival and improved the neuromuscular phenotype in treated mice.

ABSTRACT

Amyotrophic lateral sclerosis (ALS) is a relentless and fatal neurological disease characterized by the selective degeneration of motor neurons. No effective therapy is available for this disease. Several lines of evidence indicate that alteration of RNA metabolism, including microRNA (miRNA) processing, is a relevant pathogenetic factor and a possible therapeutic target for ALS.

Here, we showed that the abundance of components in the miRNA processing machinery is altered in a SOD1-linked cellular model, suggesting consequent dysregulation of miRNA biogenesis. Indeed, high-throughput sequencing of the small RNA fraction showed that among the altered miRNAs, miR-129-5p was increased in different models of SOD1-linked ALS and in peripheral blood cells of sporadic ALS patients. We demonstrated that miR-129-5p upregulation causes the downregulation of one of its targets: the RNA-binding protein ELAVL4/HuD. ELAVL4/HuD is predominantly expressed in neurons, where it controls several key neuronal mRNAs. Overexpression of pre-miR-129-1 inhibited neurite outgrowth and differentiation via HuD silencing *in vitro*, while its inhibition with an antagomir rescued the phenotype.

Remarkably, we showed that administration of an antisense oligonucleotide (ASO) inhibitor of miR-129-5p to an ALS animal model, SOD1(G93A) mice, result in a significant increase in survival and improved the neuromuscular phenotype in treated mice. These results identify miR-129-5p as a therapeutic target that is amenable to ASO modulation for the treatment of ALS patients.

Keywords (4-6): SOD-1, ALS, miRNA, therapeutic target

INTRODUCTION

Amyotrophic lateral sclerosis (ALS) is a relentless neurodegenerative disease with no effective therapeutic options. Phenotypic variability and lack of predictive models are major issues in ALS, and the need for state-specific biomarkers is therefore high. Furthermore, despite the considerable amount of data on the pathogenic mechanisms from different ALS models, a common pathophysiological mechanism that would promote meaningful therapeutic advances remains to be identified.

The genetic and environmental causes of ALS are still under investigation, but 90% of ALS cases are classified as sporadic, and only approximately 10% of patients have a familial history (1, 2). The best-studied genetic causes of ALS are mutations in or deletion of the Cu/Zn Super Oxide Dismutase 1 (*SOD1*) gene (3). Recently, using advanced genomic screening tools, researchers identified several other genes associated with ALS, including *TARDBP*, encoding TDP-43; Fused in Sarcoma (*FUS*); and *C9ORF72* (4-9). While *C9ORF72* has been identified as the most prevalent mutated gene among ALS patients, with 40% of familial ALS (fALS) patients carrying a mutation in this gene (10), the abundance and variety of identified *SOD1* mutations, which are found in 20% of fALS cases, have made this a widespread experimental paradigm (2).

Interestingly, TDP-43 and *FUS* are RNA-binding proteins that function in mRNA and miRNA biogenesis (11-13). miRNAs are small noncoding RNAs that regulate eukaryotic gene expression at the post-transcriptional level, mainly exerting a repressive function by governing the translation and degradation of target mRNAs (14). Several observations support the importance of miRNAs in neuronal physiology [reviewed in (15)]. Importantly, the disruption of miRNA expression in Purkinje cells by postnatal ablation of DICER, a crucial miRNA maturation factor, was shown to lead to neurodegeneration (16), indicating an essential role of miRNAs in the survival of differentiated post-mitotic neurons. Moreover, evidence is accumulating for a critical role of specific miRNAs in neurodegenerative disorders, as in the case of miR-206/miR-153 in Alzheimer's disease (17, 18) or miR-9/miR-9* in Huntington's disease (19). miRNA expression has also been repeatedly investigated in motor neuron (MN) diseases (6, 20-23), including ALS, where a global reduction of mature miRNAs and alterations in miRNA processing were found in *post-mortem* spinal cord samples of patients (24). In addition, specific miRNAs were found to be dysregulated in the cerebrospinal fluid, serum and leukocytes of ALS patients (25-29).

Because they regulate multiple biological processes, miRNAs have gained increasing attention as promising candidates for novel biomarkers (30-34) and therapeutic targets. Currently, several miRNA-based therapeutic strategies are being investigated for the treatment of human cancers (35). Two miRNA-based therapeutic strategies are being explored *in vivo*: the restoration of miRNA expression using miRNA mimics and inhibition with anti-miRNA molecules to block the function of the miRNA of interest. Similar approaches could be envisaged for neurodegenerative diseases, although delivery to the CNS represents an additional challenge. Nevertheless, the recent FDA approval of an antisense oligonucleotide (ASO)-based therapeutic strategy for spinal muscular atrophy (SMA) provides a successful model of intervention for other MN diseases, including ALS (36).

Here, we identified an upregulated miRNA, miR-129-5p, whose expression was consistently increased in different models of SOD1-linked ALS and in peripheral blood mononuclear cells (PBMCs) of sporadic ALS (sALS) patients. We demonstrated that miR-129-5p targets the ELAVL4 gene transcript, which encodes the RNA-binding protein HuD. HuD is predominantly expressed in neurons where it controls splicing, translation, localization, and stability of several important neuronal mRNAs [reviewed in (37)]. Overexpression of pre-miR-129-1 inhibited neurite outgrowth and differentiation via HuD silencing *in vitro*, while its inhibition with an antagomir rescued the phenotype. Importantly, we showed that administration of an ASO inhibitor of miR-129 to SOD1(G93A) mice extends survival and rescues the body weight and grip strength loss. These findings identify miR-129 as a promising therapeutic target that is amenable to ASO modulation for ALS.

MATERIALS AND METHODS

Cell lines

HEK293T cells and SH-SY5Y cells, either untransfected or stably transfected with cDNAs encoding wild type SOD1 or the mutant SOD1(G93A) (38), SH-SY5Y/miR-129-1, SH-SY5Y/Vec, NSC-34/miR-129-1, and NSC-34/Vec (39), were cultured in DMEM high-glucose medium, 10% fetal bovine serum (FBS), 2.5 mM L-glutamine, 100 U/ml penicillin, and 100 µg/ml streptomycin (all products were purchased from Euroclone) at 37°C with 5% CO₂. Stably transfected cells were maintained with 400 µg/ml gentamicin. NSC-34 cells stably transfected with the doxycycline-inducible vector for the expression of SOD1(WT) and SOD1(G93A) were maintained in F12 (Gibco, Invitrogen), 10% fetal bovine serum (FBS), 2.5 mM L-glutamine, 100 U/ml penicillin, and 100 µg/ml streptomycin at 37°C with 5% CO₂. For induction of transgenic SOD1 expression, NSC-34 cells were treated for 48 h with 2 mg/ml of doxycycline. For SH-SY5Y cell differentiation, the growth medium was exchanged 24 h after seeding for the differentiation medium consisting of DMEM high-glucose medium, 1% FBS, 2.5 mM L-glutamine, 100 U/ml penicillin, and 100 µg/ml streptomycin and 10 µM all-trans retinoic acid (RA). Differentiation medium was replaced every 2 days, and the cells were grown for up to 6–8 days.

Transfection, DNA cloning and luciferase assays

For generation of SH-SY5Y and NSC-34 cells stably expressing the miR-129-1 precursor, transfections were carried out by the classical calcium phosphate procedure. Starting 24 h post-transfection, cells were maintained in selective medium containing 0 or 4 mg/ml G418 (Gibco). For the HuD rescue experiments, a construct expressing HuD was transfected by using JetPRIME®-Polyplus transfection reagent according to the manufacturer's instructions.

MiRCURY locked nucleic acid (LNA)-inhibitor transfections were performed by using the Lipofectamine RNAi MAX system (Invitrogen, Paisley, UK) according to the manufacturer's protocol. A total of 5 x 10⁴ cells/well were seeded into 24 multiwell plates, transfected with 75 mM miR-129-5p LNA-inhibitor and collected after 48 and 72 h for SH-SY5Y and NSC34 cells, respectively.

The pre-miR-129-1-expressing plasmid pMir and the pMir Target vector carrying the HOXC10 3' untranslated region (UTR) reporter were purchased from Origene. The CACNG2 and ELAVL4/HuD 3'UTR regions were amplified using Phusion Hot Start High-Fidelity DNA Polymerase (Finnzymes) according to the manufacturer's instructions. Human genomic DNA extracted from HeLa cells was used as a template in the PCR reactions. The sequences of the oligonucleotides used in the PCR reactions are provided in Supplemental Table S1. PCR products were purified, cloned into pGEM T Easy (Promega) and sequenced. The HuD plasmid was purchased from Addgene (Plasmid #65760).

For luciferase assays, 1.5×10^5 cells/well were seeded in a 24-multiwell plate, and plasmids were transfected the following day using polyethylenimine (PEI, Sigma) according to the manufacturer's instructions. A constant amount of pRL-TK (Promega) was cotransfected with the pMiR, and the construct contained the specific 3'UTR fragment downstream of the firefly luciferase ORF. Twenty-four hours after transfection, cells were lysed in 100 μ g/well of 1x passive lysis buffer according to the manufacturer's instructions. The cells were subjected to freeze-thawing to obtain complete lysis. The luciferase assays were carried out using the Dual-Luciferase Reporter Assay System (Promega) and a Berthold luminometer (Berthold, Inc.)

Animals

Mouse spinal cords analyzed for miRNA levels were derived from transgenic mice carrying approximately 20 copies of the human SOD1 gene with the G93A mutation on the C57BL/6J strain background, and the animals were maintained at the Mario Negri Institute in compliance with institutional guidelines that comply with national (Legislative Degree 26, March 2014) and international (EEC Council Directive 2010/63, August 2013) laws and policies (40). The experiments were planned and conducted to minimize the number of animals sacrificed. Transgenic female mice were culled at 10, 15, and 22 weeks of age, corresponding to presymptomatic, onset, early symptomatic, and end-stage of the disease. Non-transgenic age-matched littermates were used as controls. RNA extraction was performed from the frozen lumbar spinal cords.

Treatment with ASOs was performed in transgenic SOD1(G93A) mice of the C57BL/6J strain carrying the same copy number as those described above, and the animals were maintained at the University of Milan (41) in compliance with the institutional guidelines. Animals studies were approved by the Mario Negri Institute Animal Care and Use Committee or the University of Milano and for the treatment with ASO by Italian Ministerial decree no. 84-2013.

Patient information

All procedures involving human participants were in accordance with the ethical standards of the institutional ethics committee and with the 1964 Helsinki Declaration and its later amendments. Ethical approval was obtained from the local committee (University of Milano-Bicocca, Italy; protocol MyoSLA 30 March 2015). Twenty-seven patients affected by sALS diagnosed according to El Escorial criteria (42) were consecutively recruited at the NEMO center (Milano, Italy) after they provided informed consent. ALS patients negative for SOD1, TARDBP, and FUS mutations and C9ORF72 hexanucleotide repeat expansions were considered eligible for the study. Table 3 shows the demographic and clinical characteristics. ALSFRS-R scores were

recorded together with the disease progression index (DPI), defined as [(48 - ALSFRS-R score at recruitment)/disease duration in months] (43). Twenty-five healthy subjects, age- and sex-matched to sALS patients, were recruited. Exclusion criteria for all the recruited subjects were cancer and autoimmune and inflammatory diseases. Moreover, healthy controls were not affected by any neurological or psychiatric condition nor were they taking psychoactive drugs.

PBMC isolation

Peripheral blood samples (15 ml) were drawn from each subject in tubes containing K₂EDTA after overnight fasting. PBMCs were collected as previously described (44). Briefly, whole blood samples were diluted with the same amount of saline solution layered on Ficoll-Histopaque (GE Healthcare) and centrifuged for 30 min at $490 \times g$ at room temperature (RT). PBMCs were collected from the interface between plasma and Ficoll-Histopaque, washed with saline solution, aliquoted and stored at -80°C .

RNA high-throughput sequencing

Human neuroblastoma SHSY-5Y cells stably transfected with cDNAs encoding wild type SOD1, with four biological replicates, or the mutant SOD1(G93A), with four biological replicates, were sequenced by whole-genome small RNA deep-sequencing (sRNAseq). In brief, total RNA was extracted using TRIzol (Invitrogen) according to the manufacturer's instructions. Samples were enriched for small RNAs up to 200 bp by size selection using a Pure Link miRNA Isolation Kit (LifeTech). RNA purity, integrity and size distribution were assessed using an Agilent 2100 Bioanalyzer (Agilent Technologies). Enriched RNA samples were processed using the Small RNA Expression Kit according to the manufacturer's protocol (Small RNA expression kit, rev. C, Applied Biosystems). RNA was first hybridized and ligated with the adapter mix "A", subsequently reverse transcribed and treated with RNase H. The obtained cDNA libraries were PCR amplified, purified and size-selected by PAGE, resulting in libraries containing inserted small RNA sequences of 20–40 bp. The size, integrity and purity of the libraries were verified by the Agilent 2100 Bioanalyzer (Agilent Technologies). cDNA libraries were barcoded using the Solid RNA barcoding kit and amplified onto beads using emulsion PCR. Templated beads were deposited on slides and analyzed using the Applied Biosystems SOLID™ 4 platform (Applied Biosystems). The quality filtered reads were trimmed to 25 nt. Filtered reads were mapped against all annotated human precursor miRNA sequences (miRBase v19.0) (45) using SHRiMP 2.0.1 (46). Mature miRNAs were extracted and reformatted with custom R scripts from the SHRIMP output. Differential expression analysis was performed with the edgeR Bioconductor statistical library (47) version 3.0.8 on R version 2.15.3.

RNA extraction and quantitative real-time PCR assays (qPCRs)

The protocols for mRNA and pri-, pre-, and mature miRNA extraction, for reverse transcription, and for the qPCR assays are provided in the Supplemental Material and Methods. The sequences of the oligonucleotide primers are listed in Supplemental Table S1.

Protein extracts and immunoblotting

Cells were washed once in 1x PBS (Euroclone) and then lysed in 0.5 ml of cold Lysis Buffer (Tris HCl 50 mM pH 7.5, 150 mM NaCl, 1% NP40, 5 mM EGTA) with protease inhibitors (Roche). The samples were incubated on ice for 20 min and centrifuged at 15000 ref for 15 min at 4°C, and the supernatants were collected. An aliquot of the cell lysate was used for protein quantification and 25 or 50 ug for each samples were loaded on. Protein were separated in 7% and 10% SDS-polyacrylamide gels in reducing conditions and transferred to nitrocellulose membranes (Whatman GmbH), in normal Transfer Buffer (25 mM Tris, 192 mM Glicine, 20% Methanol) at 100 Volts for 2h or in High Molecular Weight protein (25 mN Tris, 192 mM Glicine, 10% Methanol and 0,1% SDS) at 15 Volts overnight. Membrane were blocked using 5% non fat dried milk in PBST (0,1% (v/v) Tween 20 in 1X PBS) and incubated with the appropriate antibodies overnight at 4°C. The primary antibodies used for detection are listed in the Supplemental Materials and Methods. After washing, membranes were incubated with peroxidase- conjugated secondary antibody anti-mouse IgG (Cell signaling, 1:5000 dilution) or anti-rabbit IgG (Cell signaling 1:5000 dilution), in PBST with 5% non fat dried milk for 1h at room temperature. After washing as above, the chemo-luminescent signals developed by ECL reagents (Millipore) were detected using films. Exclusively the western blot in Figure 2F was run on a precast polyacrylamide gel (4-12%) (Invitrogen), transferred using a semi-dry system and acquired using the LI-COR Biosciences technology, Odyssey FC. In particular, secondary anti-mouse IR-DYE 800 CW (1:20000) and anti-rabbit IR-DYE 680 RD (1:20000) were added for 1-hour RT.

Immunofluorescence

Cells grown on glass coverslips were fixed with 4% PFA for 20 min and permeabilized with 0.2% Triton X-100 for 5 min. After the cells were blocked with 20% FBS in PBS with 0.05% Tween for 1 h, coverslips were incubated overnight at 4°C with Alexa Fluor phalloidin-488 (Fisher Scientific) in PBS containing 0.2% BSA. After 24 h, coverslips were washed with PBS with 0.2% BSA and incubated with anti-HuD antibody (SC48421, 1:200 dilution) for 1 h at RT. After the slides were washed, they were first incubated with anti-mouse Alexa Fluor 647 antibody (Cell Signaling) and then stained for 10 min at RT with 1 µg/ml 4,6-diamidino-2-phenylindole (DAPI, Sigma). The fluorescence 12-bit images were collected with a Leica TCS SP2 AOBS confocal microscope with the 63× oil immersion objective for pictures shown in Figure 3 and with the 40x oil immersion objective for pictures shown in Figure 4.

Morpholino treatment

The morpholino (MO) sequence targeting miR-129-1 was ACAGCAAGCCCAGACCGCAAAAAGA and was synthesized without any modifications by Gene Tools Laboratories. The ctr-MO was a standard control oligo with Morpholino chemistry provided by Gene Tools, sequence: CCT CTT ACC TCA GTT ACA ATT TAT A (Gene tools, www.gene-tools.com). MOs were dissolved in sterile saline solution at the appropriate concentration for *in vivo* experiments. All animal experiments were approved by the University of Milan and Italian Ministry of Health review boards, in compliance with US National Institutes of Health Guidelines. Adult SOD1 mice were injected with MO (40 nMoles, n = 14) or ctr-MO (n = 12) at the early symptomatic

phase (at P80) with ICV injection following the standard stereotactic coordinates. The two groups had a nearly equal representation of male and female animals.

Pathological ALS phenotype analysis after MO treatment

Neuromuscular evaluation and survival

All groups of SOD mice were monitored daily after treatment with miR-129-1 or ctr-MO sequences for phenotypic hallmarks of disease. The investigators who executed the functional assessment were blinded to the treatment. Motor function was tested weekly with a hand inverted grid test (48). Animals were placed onto a grid that was gently inverted, and latency to fall was recorded up to 60 s. The animals were sacrificed when they were unable to right themselves within 30 s when positioned in a supine position.

In vivo MN and neuromuscular junction (NMJ) count

Lumbar spinal cord and tibial anterior (TA) muscles were collected at P120 and used for histopathological analysis (n = 4/group). Serial cross sections (20 μ m thick) of the lumbar spinal cords (L1–L5) were made and stained for a specific MN marker with goat polyclonal anti-Choline Acetyl Transferase (ChAT) antibody (Millipore, 1: 125, secondary antibody, Alexa 594). The MNs in these cross sections were quantified (n = 50 per mouse). The sections were analyzed at 20 \times magnification in the ventral horn (either left or right) for the presence of all stained MNs in that region. TA muscles were cryosectioned (20 μ m) and stained for NMJ detection and count. All sections were saturated with 10% bovine serum albumin and 0.3% Triton X-100 for 1 h at RT before incubation with rabbit Neurofilament Medium (NF-M, Millipore 1:250) overnight at 4°C. The next day, the slides were incubated with Alexa Fluor 488 (1:1000; Life Technologies) and α bungarotoxin 555 (1:500, Life Technologies). A minimum of 100 NMJs from each muscle were randomly selected, and the number of denervated/degenerated NMJs was determined for each muscle group in each animal based on NF-M/ α BTX staining.

Statistical analysis

All statistical analyses were performed with Excel and GraphPad Prism. For multiple comparisons on a single data set, one-way analysis of variance (ANOVA) was used, and when several variables were taken into account, two-way ANOVA was used, followed by appropriate post hoc analysis. Two-tailed, unpaired Student's t test was used to compare two groups. Kaplan–Meier survival analysis and the log-rank test were used for survival comparisons, while the contingency chi-square test was applied to the NMJ count. The data met the assumptions of the specific statistical tests chosen, and $*p \leq 0.05$, $**p \leq 0.01$, and $***p \leq 0.001$ were considered significant. All experiments were performed minimally in triplicate. Individual statistical tests are detailed in the figure legends. All results are expressed as the mean \pm SEM or mean \pm SD. Western blot images were analyzed using ImageJ software (49). The value of each band was normalized to the intensity of the corresponding housekeeping band, thus obtaining relative intensity values. In the qPCR experiments, for relative quantification of each target vs. housekeeping mRNA, the comparative CT method was used as previously described (50).

RESULTS

miR-129-5p is upregulated in human and mouse models of SOD1-linked ALS and in PBMCs of sALS patients.

Dysregulated miRNA biogenesis and expression is a key pathogenetic element in ALS pathogenesis. To thoroughly investigate this phenomenon, we analyzed the expression levels of the components in the miRNA processing apparatus in an ALS SOD1-linked cellular model.

We compared the abundance of components in the miRNA biogenesis machinery between human neuroblastoma SH-SY5Y cells stably expressing either the wild type SOD1 (SH-SY5Y/SOD1 cells) or the mutant SOD1(G93A) protein [SH-SY5Y/SOD1(G93A) cells] (38). Western blot analysis showed a significant downregulation of DROSHA and its cofactor DGCR8, which process pri-miRNA into pre-miRNA, in SOD1(G93A) cells compared to cells expressing the wild type SOD1 protein (Figure 1A). Intriguingly, we also found a 2- to 3-fold increase in the expression of DICER, the RNase III enzyme that processes pre-miRNA to mature miRNA in the cytosol (Figure 1A). Because DROSHA expression was shown to be negatively regulated by Ewing Sarcoma protein (EWS) (43), we also analyzed EWS, FUS and TDP-43 protein levels in SOD1(G93A) cells (Figure 1B). While neither the TDP-43 nor FUS levels changed, the EWS RNA binding protein was strongly upregulated, which is consistent with the observed downregulation of DROSHA.

Overall, our results indicated that expression of the mutant SOD1(G93A) protein affects the abundance of components in the miRNA processing machinery, suggesting that the miRNA transcriptome might also be altered in SOD1(G93A) cells.

To test this hypothesis, we performed high-throughput sequencing of the small RNA fraction (miRNAseq) of SH-SY5Y/SOD1 and SH-SY5Y/SOD1(G93A) cells and identified nine differentially expressed miRNAs (Table 1). In addition, we used the T-REX algorithm [from Targets' Reverse Expression, (51)] to predict additional miRNAs affected by the expression of the mutant SOD1 protein based on our previous microarray profiling of SH-SY5Y/SOD1 and SH-SY5Y/SOD1(G93A) cells (52). Based on the results of these two approaches, we compiled a panel of 27 miRNAs that were validated by quantitative real-time RT-PCR (qRT-PCR, Supplemental Figure S1A). We identified four significantly downregulated miRNAs (miR-29b, miR-30c, miR-30-e, and miR-124) and three significantly upregulated miRNAs (miR-29c, miR-129-5p, and miR-200c). Interestingly, the miRNA showing the strongest downregulation, miR-124 (0.2-fold change), plays a well-described role in neuronal differentiation (15).

To determine if the effect of mutant SOD1 protein expression on the miRNA transcriptome was observed *in vivo* and to identify consistently affected miRNAs, we selected a panel of 20 of the 27 miRNAs based on their known roles in neuronal and neurodegenerative pathways for further analysis in the spinal cord of a SOD1(G93A) mouse model. While the expression of the majority of the analyzed miRNAs was either unchanged or not significantly affected at the pre-onset (10 weeks) and symptomatic stage (22 weeks) of the disease (Supplemental Figure S1B), miR-129-5p and miR-200c were upregulated at the early symptomatic

stage (15 weeks, Supplemental Figure S1B). Consistent with the report of Williams *et al.* (6), miR-206 was also upregulated in all the stages examined. Based on these results, we increased the subset of mice at this stage of disease to measure the expression of miR-129-5p and miR-200c and miR-30c as a control miRNA whose level was not affected by the mutation. While the upregulation of miR-129-5p was confirmed, the expression of miR-200c could be detected in only three of the seven samples that were analyzed, (Figure 1C). MiRNAs circulating in the blood, either in cell-free plasma or in PBMCs, are currently under evaluation as potential biomarkers not only in cancer but also in neurodegenerative pathologies. Thus, we analyzed the expression of the conserved miRNAs in PBMCs obtained from a small group of sALS patients. Although only seven of the 20 miRNAs analyzed could be detected and reliably quantified in these PBMC samples, this analysis confirmed the upregulation of miR-129-5p and miR-200c (Supplemental Figure S1C). We therefore measured miR-129-5p and miR-200c levels, along with miR-30c as a negative control, in a larger cohort of sALS patients (Table 2) and found that miR-129-5p was on average increased by twofold ($p < 0.001$, t test) and miR-200c by almost threefold ($p < 0.001$, t test) in sALS patients compared to controls (Figure 1D). No influence on the demographic and clinical characteristics of the recruited subjects was observed on any of the investigated parameters. No significant difference was found in all evaluated parameters by dichotomizing ALS patients based on the site of onset, presence of percutaneous endoscopic gastrostomy (PEG) or non-invasive ventilation (NIV), and riluzole treatment.

Overall, the analysis of miRNA expression in *in vitro* and *in vivo* models of SOD1(G93A)-linked ALS and in sALS patients revealed an association between a high abundance of specific miRNAs and ALS pathogenesis, suggesting the presence of a common mechanism underlying the disease.

Overexpression of pre-miR-129-1 inhibits neurite outgrowth and differentiation via HuD silencing

Since miR-129-5p was upregulated in all our ALS disease paradigms, we focused on this miRNA to identify its putative target genes and characterize their roles in ALS onset and progression.

We used the prediction algorithm DIANA-microT to identify ALS-related potential target genes for miR-129-5p. Among the top ranking putative targets, *CACNG2*, *ELAVL4*, and *HOXC10* were selected for experimental validation. *CACNG2* (calcium channel, voltage-dependent, gamma subunit 2), also known as stargazin, is involved in the transport of AMPA receptors to the synaptic membrane and the regulation of their receptor rate constant (53). *ELAVL4*, also known as HuD, plays a well-characterized role in neuronal cell identity, maturation and survival (37). In addition, adult HuD-deficient mice exhibited an abnormal hind limb reflex and poor rotarod performance, resembling those found in MN disease (54). *HOXC10* belongs to the homeobox family of transcription factors and is involved in MN differentiation (55).

To investigate whether *CACNG2*, HuD, and *HOXC10* can be directly targeted by miR-129-5p, we generated luciferase reporter constructs containing the 3'UTRs of these three human genes. After transfection of the reporters into HEK293 cells stably expressing the precursor of miR-129-5p, miR-129-1, a significant repression of luciferase activity was observed for all 3'UTR reporters (Figure 2A). We further examined whether miR-129-5p repressed the expression of the endogenous *CACNG2*, *HuD*, and *HOXC10* genes in SH-

SY5Y cells stably expressing the precursor miR-129-1 (termed SH-SY5Y/miR-129-1, Supplemental Figure S2A for quantification of the expression level of the exogenous miR) (Figure 2B). Western blot analysis showed a strong reduction of HuD expression, while the CACNG2 protein level was only slightly diminished. In contrast, we observed increased expression of HOXC10. These observations suggest that only HuD is a *bona fide* target of miR-129. To confirm this result, we generated mouse MN-like NSC-34 cells stably overexpressing miR-129-1 (NSC-34/miR-129-1), which also showed a significant decrease in HuD protein by ~40% (Supplemental Figure S2B). Moreover, we mutated the miR-129-5p binding site in the HuD 3'-UTR and performed a luciferase reporter assay. We found that miR-129 did not affect luciferase activity controlled by mutant HuD UTR (Supplemental Figure S2C). We further analyzed endogenous HuD expression in SH-SY5Y/SOD1(G93A) cells, observing a specific reduction in HuD expression (Figure 2C). An even stronger reduction of HuD expression was observed in an inducible system of NSC-34 cells engineered to express either human SOD1(G93A) mutant protein or the wild type SOD1 protein the upon doxycycline treatment (56) (Figure 2D), consistent with a two-fold increase of miR-129-5p ($p < 0.05$) in the NSC-34/ SOD1(G93A) cells (Supplemental Figure S2D).

Next, we tested whether depletion of miR-129-5p leads to an increase in HuD protein. To this end, we transfected either a scrambled or a miR-129-5p LNA oligonucleotide inhibitor in SH-SY5Y/miR-129-1 and NSC-34/miR-129-1 cells to bind and sequester the free miRNA. As shown in Figure 2E, in both cell lines, LNA-mediated anti-miR-129-5p silencing resulted in increased expression of HuD. Overall, these results support the conclusion that HuD expression is regulated by miR-129-5p. To further confirm our hypothesis, we investigated HuD levels in early phase SOD1(G93A) murine spinal cord compared to wild-type murine spinal cord and we observed a significant downregulation in the first group (Figure 2F, $p < 0.05$).

Intriguingly, HuD was shown to play crucial roles in neuronal development, particularly in controlling neuritogenesis *in vivo* (54, 57). To assess the effect of miR-129-5p on neuronal differentiation, we assessed neurite outgrowth in control and SH-SY5Y/miR-129-1 cells treated with 10 μ M RA. While control cells showed long branching processes, SH-SY5Y/miR-129-1 cells developed short, improperly formed neurite projections (Figure 3A). We also examined the expression of the neuronal markers NEUROD1, tubulin beta III (TUBB3) and MAP2, as well as ASCL1, a marker of neuroblasts (58). RT-qPCR analysis showed a significant decrease in all three neuronal markers and an upregulation of *ASCL1* in SH-SY5Y/miR-129-1 cells (Figure 3B). In addition, we measured the mRNA levels of three known HuD targets that function in neuronal differentiation [*musashi*, *MSH1* (59)] and neurite extension [*GAP43* (60) and *Tau/MAPT* (61)] that are stabilized by HuD (37). Consistent with the idea that miR-129-5p inhibits neuronal differentiation through HuD targeting, significant downregulation of these three HuD-regulated transcripts was observed (Figure 3C). Finally, to verify that the impaired differentiation of SH-SY5Y/miR-129-1 cells was due to the miR-129-mediated silencing of HuD expression, we transiently transfected cells with a plasmid expressing the HuD ORF lacking the miR-129-1 binding site. As shown in Figure 3D, 3E and Supplemental Figure 2E, SH-SY5Y/miR-129-1 cells expressing exogenous miR-129-1-insensitive HuD mRNA showed restored HuD

protein levels and displayed robust neurite outgrowth in response to RA. In contrast, mock-transfected SH-SY5Y/miR-129-1 cells displayed low levels of HuD protein and showed a rounded appearance with few, very short neurites. Taken together, these results demonstrated that miR-129-5p regulates neurite formation by modulating HuD expression, which is important in ALS pathogenesis.

miR-129 silencing improves the neurological phenotype and survival in SOD1(G93A) mice

We next evaluated whether the inhibition of miRNA-129-5p significantly alleviated the disease phenotype of an ALS mouse model [SOD1(G93A) mice]. Given its safety, efficacy and optimal translational profile, MO chemistry was used to synthesize a specific ASO to block the miR-129-5p precursor, miR-129-1. We first tested the ability of MO in decreasing miR-129 expression level, treating wild-type pups intracerebroventricularly (ICV) with 24 nmoles of MO and we harvested spinal cords after 1 week. RT-qPCR analysis showed a significant decrease of miR-129-5p expression levels after treatment (n=4/groups, $p < 0.01$, Supplemental Figure S3A), demonstrating the efficacy of MO sequence. Accordingly, we also measured a significant ($p < 0.05$) increase in HuD protein level in the same mice (Supplemental Figure S3B).

We injected MO into the cerebrospinal fluid (CSF) of SOD1(G93A) mice (MO-SOD1 mice) at the early disease stage [post-natal day 80 (P80)] by intracerebroventricular injection (48). No major side effects were observed after treatment.

Remarkably, we observed a significant increase in the lifespan of MO-treated SOD1 mice. The median ages at death were 180 days for MO-treated SOD1 mice (n = 14) and 160 days (n = 12) for ctr-treated mice (ctr-SOD mice) ($\chi^2 = 7.232$, $p = 0.0072$, Kaplan–Meier log-rank test) (Figure 4A). The median survival of our SOD1(G93A) colony without any treatment is 153 ± 6 days. MO-SOD1 mice showed increased muscle strength compared to ctr-SOD1 mice, as shown by a significant improvement in the inverted grid assay at the symptomatic disease stages. Data were evaluated by two-way ANOVA for repeated measures ($p = 0.0048$, for treatment factor; Figure 4B). Since ALS is characterized by progressive MN degeneration, we determined the MN number through histological analysis of spinal cord sections of the lumbar L1-L5 region, which is the most affected district in SOD1(G93A) mice at 120 days of age. We observed a trend toward reduced MN loss after MO administration, although this change was not statistically significant (Figure 4C).

NMJ denervation, axon degeneration and collateral sprouting for the remaining MNs are all pathological hallmarks of ALS. The typical progressive irreversible muscle paralysis is due to the increasing loss of MNs that is associated with the retraction of axons from NMJs, which is not sufficiently compensated by the axonal collateral sprouts from surviving MNs. Interestingly, MO-treated SOD1(G93A) mice showed a significant increase in the number of fully innervated NMJs compared to scr-SOD1 mice (Figure 4D and E, $p < 0.05$, $\chi^2 = 4.153$), indicating that the MO treatment significantly counteracted NMJ degeneration with a recovery of peripheral synapses. In particular, the average of denervated NMJ is $74/100 \pm 7.39$ for MO-SOD treated mice and $90/100 \pm 1.91$ for ctr-SOD1-treated mice. The difference between the two means is statistically significant, $p < 0.05$ (data not shown).

Overall, these results demonstrated the therapeutic efficacy of miR-129-1 silencing in ameliorating the murine ALS pathological phenotype, identifying the miR-129 pathway as a potential therapeutic target suitable for ASO modulation for the treatment of ALS patients.

DISCUSSION

In the present study, we showed that miR-129-5p is upregulated in familial SOD1-linked ALS and in sALS, where it suppresses HuD expression and impairs neurite formation. Moreover, inhibition of miR-129-5p with an antagomir restored neurogenesis *in vitro* and ameliorated survival and neuromuscular function when administered in the CSF of SOD1(G93A) mice *in vivo*.

Since their discovery, more than 2500 miRNAs have been identified in human cells according to the most recent release of the miRBase reference database (62). miRNAs play a central role in multiple biological processes and pathways that are important in both normal and diseased states. Their function in disease has been particularly investigated in human cancers, and various miRNA-based therapeutics are currently being explored to modulate their expression (63). In the nervous system, miRNAs are required for the survival of specific types of mature neurons in model organisms (64). Moreover, the conditional ablation of Dicer, a crucial component of the miRNA processing machinery, causes degeneration and death of various types of neurons in mice (20, 64-66), supporting the idea that abnormal miRNA expression can contribute to the etiology or progression of neurodegenerative disorders.

In ALS, the involvement of miRNAs is supported by several observations. TDP-43 and FUS interact with components of the miRNA processing complexes, thereby affecting miRNA expression (11, 67) (13, 68). Importantly, DROSHA was found in the cytoplasmic protein aggregates in *post mortem* brain samples of frontotemporal lobar degeneration (FTLD) and ALS cases with C9ORF72 mutations and TDP-43 pathology (69). Several studies have also reported altered miRNA expression in SOD1-linked ALS models (70, 71) (72), as well as in SOD1 fALS, and in sALS patients (22, 27). However, no consistent changes have emerged thus far. Rather, the pool of dysregulated miRNAs may differ in the presymptomatic and symptomatic stages of the disease (73, 74), while a general downregulation of miRNAs has consistently been observed in *post mortem* spinal cord tissue of sALS and fALS patients (24, 75) and in the late symptomatic SOD1(G93A) mice (23). miR-129-5p is highly expressed in the human brain and spinal cord [Supplemental Figure S4 (76)] and is particularly enriched in synaptosomal preparations (77). Despite these observations, very little is known about its function in the nervous system. We identified the RNA-binding protein HuD as a target of miR-129-5p by bioinformatic analysis and then experimentally validated the results. Indeed, the HuD protein was downregulated in human SH-SY5Y and in mouse NSC-34 cells overexpressing the miR-129-1 precursor. miR-129-5p overexpression in SH-SY5Y and in NSC-34 cells inhibited the expression of neuronal differentiation markers and neurite outgrowth, a phenomenon that notably also occurred in cells overexpressing the mutant SOD1 protein, in which HuD is downregulated. Our results are particularly intriguing in light of the early reduction in dendritic arbor length of vulnerable lumbar spinal cord MNs of SOD1(G93A) mice (78) and of the loss of intraepidermal nerve fibers (the terminal endings of small-diameter sensory neurons located in

dorsal root ganglia) that was observed in 75% of sALS and fALS patients (79, 80) and in presymptomatic SOD1(G93A) mice (40).

Our results showed that HuD expression is reduced in cells and animals expressing the pathogenic SOD1(G93A) mutation and that administration of an antagomir of miR-129-5p rescues HuD expression *in vitro*. HuD plays a fundamental role in controlling neuronal cell fate by stimulating the translation of mRNAs involved in neuronal cell commitment and axonogenesis (81). HuD has previously been linked to neurodegeneration and MN function. In the hippocampus of Alzheimer's disease patients, a decrease in HuD protein levels correlated with dementia progression (82). Moreover, three separate studies have linked SNPs within the HuD locus to the development of Parkinson's disease (83-85). The pivotal role of HuD in neuronal homeostasis is also suggested by the demonstration that prenatal knockout in mice disrupts the correct establishment and functioning of neocortical and hippocampal circuitry (57) and, importantly, results in MN deficits, resembling a MN disease (54). HuD interacts with the SMN protein in the axonal compartments of neurons (86-89), is essential for motor neuron development and function (89), and was reported to interact and be sequestered in TDP-43 inclusions in MN cell bodies and neurites (90). Recently, De Santis et al. reported the upregulation and aggregation of HuD in FUS-linked ALS (91). Importantly, these authors observed that HuD is a common component of FUS-positive and TDP-43-positive neuronal cytoplasmic inclusions, in FUS and sporadic ALS patients (91). Since HuD sequestration in cytoplasmic inclusions may lead to a depletion of nuclear HuD or other types of HuD loss of function, we hypothesize that HuD deficiency may be a common trait in ALS.

In the second part of our study, we showed that CSF administration of MO against the miR-129 precursor significantly ameliorated the ALS phenotype in a rodent disease model. The therapeutic effects of MO included statistically significant improvements in neuromuscular function and survival and the protection of host MNs and NMJ innervation, as shown by neuropathological analyses. The increase of the survival observed is highly meaningful in the context of SOD1G93A mice, since in this model the phenotype modification and life-span extension are difficult to achieve by therapeutic approaches besides directly targeting the mutant SOD1 protein. Interestingly, the therapeutic effect was more pronounced on NMJ innervation than on MN cell number increase, suggesting that muscles in MO-SOD1 mice were reinnervated by terminal and collateral sprouts elongating from resistant MNs and/or that the spare NMJs were preserved. This specific effect can be correlated with the role of the miR-129 target HuD. Indeed, axonal regeneration following peripheral axon injury was associated with increased levels of HuD and its direct target GAP43 (92). In addition, HuD was shown to restore axon outgrowth defects in SMA MNs (86). Further studies are needed to confirm the role of HuD protein in axonal homeostasis. Importantly, the MO administration was well tolerated, and no major side effects were observed in treated mice. We cannot exclude that the miR-129 effect is due to cells other than neurons (such as astrocytes or microglia). However, previous *in situ* hybridization experiments on the rodent spinal cord suggest that miR-129, particularly miR-129-1, is predominantly expressed in both the cytoplasm and in the nucleus of the neuropil and large neuronal cells (93). These *in vivo* results are crucially important for the development of a potential therapeutic approach for ALS patients. Indeed, the recent approval of the

ASO Spinraza for SMA therapy (94) is a strong proof-of-principle that ASOs can be used to target the CNS for the treatment of neurological diseases. ASOs show widespread distribution in the brain and spinal cord after CSF administration using intraventricular or intrathecal injections. ASO delivery into the CSF by lumbar puncture has already been implemented in human clinical trials for ALS and other neurodegenerative diseases (95). ASOs have an advantage as their effects on gene expression are reversible, which is particularly important for side effects, and so have a safer profile than gene therapy approaches where the genetic modification is permanent.

Notably, we observed significant positive results with ASOs even if animals were treated after the onset of disease symptoms, yet still in the early symptomatic stages. This outcome is relevant given that human trials will likely be performed in symptomatic patients.

Our proof-of-concept findings reported here suggest the clinical benefit for ALS patients of HuD targeting, given its axogenetic properties (81), to maintain the axon connection with the muscles and to promote the ability of MNs to form new NMJs via collateral sprouting maintaining the functional motor unit.

As an alternative therapeutic strategy, the combined silencing of miR-129 and other miRNA, already studied in ALS, can be considered, as their mechanisms of action are likely synergistic. A likely candidate could be miR-155 because of its function, mostly related to CNS inflammation through its ability to regulate microglia. Koval et al. demonstrated that widespread microRNA-155 inhibition with oligonucleotide-based miRNA inhibitors prolongs survival in ALS-model mice 9.5 days (7% increase) (96). Butovsky et al. confirmed this improvement after miRNA-155 peripheral inhibition with locked nucleic acid (LNA) (11 days, 8% increase in survival, 97). Specifically, this group examined miRNA expression in the spinal cord microglia of SOD1 mice and in PBMCs of sALS patients, observing an increase in a subset of miRNAs that have been associated with inflammatory responses. Since in our work we demonstrated that miR-129 inhibition resulted in a higher survival extension of 20 days (12.5% increase), we propose that the combination of the two miRNA would increase therapeutic efficacy.

Overall, this study provides new insights into ALS pathology and identifies miR-129-5p and HuD as possible therapeutic targets for the development of novel meaningful treatment strategies for ALS patients.

AUTHOR CONTRIBUTIONS

A.L. conceived and performed the experiments and the data analysis for Figures 1, 2, 3 and associated supplementary data and participated in preparing figures and tables. M.N. conducted the *in vivo* MO studies and provided data for Figure 4 and participated in the manuscript writing. A.A. conducted the mice studies and provided data thereof. M-D.R. performed the experiment in Figure S1A. R.A.C. was responsible for miRNA-seq and data analysis. S.V. performed the T-REX analysis and bioinformatics analysis of miRNA targets. M.R. performed the histological analysis on SOD1 mice and the experiment and data analysis for Figure S3. C.B. provided mouse RNA from the spinal cord at different disease stages. C.F., A.R., and O.M. critically revised the manuscript. C.L. and L.T. selected and characterized patients and provided lymphocytes.

S.M.L.B., S.C., and L.T. conceived the study and wrote the manuscript. All coauthors provided discussion and data interpretation and contributed to the final version of the manuscript.

Ethical approval

All procedures performed in studies involving human participants were in accordance with the ethical standards of the institutional and/or national research committee and with the 1964 Helsinki Declaration and its later amendments or comparable ethical standards.

All applicable international, national, and/or institutional guidelines for the care and use of animals were followed. All procedures performed in studies involving animals were in accordance with the ethical standards of the institution or practice at which the studies were conducted.

CONFLICT OF INTERESTS

The authors have no competing interest.

ACKNOWLEDGMENTS

We would like to dedicate this paper to the memory of Maria Teresa Carri and thank her for her precious contribution to the ALS field. We are in debt to the patients and their families for their participation in this project. We also thank the Italian Association for ALS (AISLA) for their continuous support and G. Meister, T. Treiber and N. Treiber for technical assistance. We thank A. Poletti for the kind gift of NSC-34/SOD1 and NSC-34/SOD1(G93A) cells and M.T. Carri' for the SOD1(G93A) mouse RNA. We are indebted to S. Penco, C. Tarlarini, and L. Mosca for the genetic data, F. Gerardi for the clinical data and V. Melzi for the qPCR setting. "MiRALS" and "smallRNALS" ARISLA Grant to SB and SC and (TRANS-ALS) - Regione Lombardia (no. 2015-0023) to SC and CB are gratefully acknowledged. We thank the Associazione del Centro Dino Ferrari for their support. The work was partially funded by the Ministry of Health (to M.N. and S.C.).

References

1. R. Chia, A. Chio, B. J. Traynor, Novel genes associated with amyotrophic lateral sclerosis: diagnostic and clinical implications. *The Lancet. Neurology* **17**, 94 (Jan, 2018).
2. A. E. Renton, A. Chio, B. J. Traynor, State of play in amyotrophic lateral sclerosis genetics. *Nature neuroscience* **17**, 17 (Jan, 2014).
3. D. R. Rosen *et al.*, Mutations in Cu/Zn superoxide dismutase gene are associated with familial amyotrophic lateral sclerosis. *Nature* **362**, 59 (Mar 4, 1993).
4. M. DeJesus-Hernandez *et al.*, Expanded GGGGCC hexanucleotide repeat in noncoding region of C9ORF72 causes chromosome 9p-linked FTD and ALS. *Neuron* **72**, 245 (Oct 20, 2011).
5. T. J. Kwiatkowski, Jr. *et al.*, Mutations in the FUS/TLS gene on chromosome 16 cause familial amyotrophic lateral sclerosis. *Science* **323**, 1205 (Feb 27, 2009).
6. C. Vance *et al.*, Mutations in FUS, an RNA processing protein, cause familial amyotrophic lateral sclerosis type 6. *Science (New York, N.Y.)* **323**, 1208 (Feb 27, 2009).
7. A. Yokoseki *et al.*, TDP-43 mutation in familial amyotrophic lateral sclerosis. *Annals of neurology* **63**, 538 (Apr, 2008).
8. E. Kabashi *et al.*, TARDBP mutations in individuals with sporadic and familial amyotrophic lateral sclerosis. *Nature genetics* **40**, 572 (May, 2008).
9. J. Sreedharan *et al.*, TDP-43 mutations in familial and sporadic amyotrophic lateral sclerosis. *Science (New York, N.Y.)* **319**, 1668 (Mar 21, 2008).
10. E. Majounie *et al.*, Frequency of the C9orf72 hexanucleotide repeat expansion in patients with amyotrophic lateral sclerosis and frontotemporal dementia: a cross-sectional study. *The Lancet. Neurology* **11**, 323 (Apr, 2012).
11. Y. Kawahara, A. Mieda-Sato, TDP-43 promotes microRNA biogenesis as a component of the Drosha and Dicer complexes. *Proceedings of the National Academy of Sciences of the United States of America* **109**, 3347 (Feb 28, 2012).
12. E. Buratti *et al.*, Nuclear factor TDP-43 can affect selected microRNA levels. *Febs J* **277**, 2268 (May, 2010).
13. M. Morlando *et al.*, FUS stimulates microRNA biogenesis by facilitating co-transcriptional Drosha recruitment. *The EMBO journal* **31**, 4502 (Dec 12, 2012).
14. A. Loffreda, A. Rigamonti, S. M. Barabino, S. C. Lenzken, RNA-Binding Proteins in the Regulation of miRNA Activity: A Focus on Neuronal Functions. *Biomolecules* **5**, 2363 (2015).
15. A. X. Sun, G. R. Crabtree, A. S. Yoo, MicroRNAs: regulators of neuronal fate. *Current opinion in cell biology* **25**, 215 (Apr, 2013).
16. A. Schaefer *et al.*, Cerebellar neurodegeneration in the absence of microRNAs. *The Journal of experimental medicine* **204**, 1553 (Jul 9, 2007).
17. S. T. Lee *et al.*, miR-206 regulates brain-derived neurotrophic factor in Alzheimer disease model. *Annals of neurology* **72**, 269 (Aug, 2012).
18. C. Liang *et al.*, MicroRNA-153 negatively regulates the expression of amyloid precursor protein and amyloid precursor-like protein 2. *Brain research* **1455**, 103 (May 21, 2012).
19. A. N. Packer, Y. Xing, S. Q. Harper, L. Jones, B. L. Davidson, The bifunctional microRNA miR-9/miR-9* regulates REST and CoREST and is downregulated in Huntington's disease. *The Journal of neuroscience : the official journal of the Society for Neuroscience* **28**, 14341 (Dec 31, 2008).
20. S. Haramati *et al.*, miRNA malfunction causes spinal motor neuron disease. *Proc Natl Acad Sci U S A* **107**, 13111 (Jul 20, 2010).
21. C. Parisi *et al.*, MicroRNA-125b regulates microglia activation and motor neuron death in ALS. *Cell death and differentiation* **23**, 531 (Mar, 2016).
22. O. Butovsky *et al.*, Targeting miR-155 restores abnormal microglia and attenuates disease in SOD1 mice. *Annals of neurology* **77**, 75 (Jan, 2015).
23. A. Emde *et al.*, Dysregulated miRNA biogenesis downstream of cellular stress and ALS-causing mutations: a new mechanism for ALS. *The EMBO journal* **34**, 2633 (Nov 3, 2015).
24. C. Figueroa-Romero *et al.*, Expression of microRNAs in human post-mortem amyotrophic lateral sclerosis spinal cords provides insight into disease mechanisms. *Molecular and cellular neurosciences* **71**, 34 (Mar, 2016).

25. M. Benigni *et al.*, Identification of miRNAs as Potential Biomarkers in Cerebrospinal Fluid from Amyotrophic Lateral Sclerosis Patients. *Neuromolecular medicine*, (Apr 27, 2016).
26. B. De Felice *et al.*, miR-338-3p is over-expressed in blood, CFS, serum and spinal cord from sporadic amyotrophic lateral sclerosis patients. *Neurogenetics* **15**, 243 (Oct, 2014).
27. I. Takahashi *et al.*, Identification of plasma microRNAs as a biomarker of sporadic Amyotrophic Lateral Sclerosis. *Molecular brain* **8**, 67 (2015).
28. A. Freischmidt *et al.*, Serum microRNAs in sporadic amyotrophic lateral sclerosis. *Neurobiology of aging* **36**, 2660 e15 (Sep, 2015).
29. E. Tasca, V. Pegoraro, A. Merico, C. Angelini, Circulating microRNAs as biomarkers of muscle differentiation and atrophy in ALS. *Clinical neuropathology* **35**, 22 (Jan-Feb, 2016).
30. P. M. Gaughwin *et al.*, Hsa-miR-34b is a plasma-stable microRNA that is elevated in pre-manifest Huntington's disease. *Human molecular genetics* **20**, 2225 (Jun 1, 2011).
31. M. Miyachi *et al.*, Circulating muscle-specific microRNA, miR-206, as a potential diagnostic marker for rhabdomyosarcoma. *Biochemical and biophysical research communications* **400**, 89 (Sep 10, 2010).
32. D. Galimberti *et al.*, Circulating miRNAs as potential biomarkers in Alzheimer's disease. *Journal of Alzheimer's disease : JAD* **42**, 1261 (2014).
33. A. Keller *et al.*, Stable serum miRNA profiles as potential tool for non-invasive lung cancer diagnosis. *RNA biology* **8**, 506 (May-Jun, 2011).
34. F. Cloutier, A. Marrero, C. O'Connell, P. Morin, Jr., MicroRNAs as potential circulating biomarkers for amyotrophic lateral sclerosis. *Journal of molecular neuroscience : MN* **56**, 102 (May, 2015).
35. R. Rupaimoole, F. J. Slack, MicroRNA therapeutics: towards a new era for the management of cancer and other diseases. *Nature reviews. Drug discovery* **16**, 203 (Mar, 2017).
36. V. Parente, S. Corti, Advances in spinal muscular atrophy therapeutics. *Therapeutic advances in neurological disorders* **11**, 1756285618754501 (2018).
37. L. M. Bronicki, B. J. Jasmin, Emerging complexity of the HuD/ELAVI4 gene; implications for neuronal development, function, and dysfunction. *RNA (New York, N.Y.)* **19**, 1019 (Aug, 2013).
38. M. T. Carri *et al.*, Expression of a Cu,Zn superoxide dismutase typical of familial amyotrophic lateral sclerosis induces mitochondrial alteration and increase of cytosolic Ca²⁺ concentration in transfected neuroblastoma SH-SY5Y cells. *FEBS letters* **414**, 365 (Sep 8, 1997).
39. E. Babetto *et al.*, Tetracycline-regulated gene expression in the NSC-34-tTA cell line for investigation of motor neuron diseases. *Brain research. Molecular brain research* **140**, 63 (Oct 31, 2005).
40. J. Sassone *et al.*, ALS mouse model SOD1G93A displays early pathology of sensory small fibers associated to accumulation of a neurotoxic splice variant of peripherin. *Human molecular genetics* **25**, 1588 (Apr 15, 2016).
41. M. E. Gurney *et al.*, Motor neuron degeneration in mice that express a human Cu,Zn superoxide dismutase mutation. *Science* **264**, 1772 (Jun 17, 1994).
42. B. R. Brooks, R. G. Miller, M. Swash, T. L. Munsat, El Escorial revisited: revised criteria for the diagnosis of amyotrophic lateral sclerosis. *Amyotrophic lateral sclerosis and other motor neuron disorders : official publication of the World Federation of Neurology, Research Group on Motor Neuron Diseases* **1**, 293 (Dec, 2000).
43. L. Tremolizzo, C. Ferrarese, I. Appollonio, Exploring limits of neuropsychological screening in ALS: the FAB problem. *Amyotrophic lateral sclerosis & frontotemporal degeneration* **14**, 157 (Mar, 2013).
44. A. Arosio *et al.*, MEF2D and MEF2C pathways disruption in sporadic and familial ALS patients. *Molecular and cellular neurosciences* **74**, 10 (Jul, 2016).
45. S. Griffiths-Jones, H. K. Saini, S. van Dongen, A. J. Enright, miRBase: tools for microRNA genomics. *Nucleic acids research* **36**, D154 (Jan, 2008).
46. S. M. Rumble *et al.*, SHRiMP: accurate mapping of short color-space reads. *PLoS computational biology* **5**, e1000386 (May, 2009).
47. M. D. Robinson, A. Oshlack, A scaling normalization method for differential expression analysis of RNA-seq data. *Genome biology* **11**, R25 (2010).
48. M. Nizzardo *et al.*, Morpholino-mediated SOD1 reduction ameliorates an amyotrophic lateral sclerosis disease phenotype. *Scientific reports* **6**, 21301 (Feb 16, 2016).
49. C. A. Schneider, W. S. Rasband, K. W. Eliceiri, NIH Image to ImageJ: 25 years of image analysis. *Nature methods* **9**, 671 (Jul, 2012).

50. G. Sala *et al.*, Vesicular monoamine transporter 2 mRNA levels are reduced in platelets from patients with Parkinson's disease. *Journal of neural transmission (Vienna, Austria : 1996)* **117**, 1093 (Sep, 2010).
51. S. Volinia, R. Visone, M. Galasso, E. Rossi, C. M. Croce, Identification of microRNA activity by Targets' Reverse EXpression. *Bioinformatics (Oxford, England)* **26**, 91 (Jan 1, 2010).
52. S. C. Lenzken *et al.*, Mutant SOD1 and mitochondrial damage alter expression and splicing of genes controlling neuritogenesis in models of neurodegeneration. *Hum Mutat* **32**, 168 (Feb, 2011).
53. L. Chen *et al.*, Stargazin regulates synaptic targeting of AMPA receptors by two distinct mechanisms. *Nature* **408**, 936 (Dec 21-28, 2000).
54. W. Akamatsu *et al.*, The RNA-binding protein HuD regulates neuronal cell identity and maturation. *Proceedings of the National Academy of Sciences of the United States of America* **102**, 4625 (Mar 22, 2005).
55. Y. Wu, G. Wang, S. A. Scott, M. R. Capecchi, Hoxc10 and Hoxd10 regulate mouse columnar, divisional and motor pool identity of lumbar motoneurons. *Development* **135**, 171 (Jan, 2008).
56. T. Prell, J. Lautenschlager, O. W. Witte, M. T. Carri, J. Grosskreutz, The unfolded protein response in models of human mutant G93A amyotrophic lateral sclerosis. *The European journal of neuroscience* **35**, 652 (Mar, 2012).
57. E. M. DeBoer *et al.*, Prenatal deletion of the RNA-binding protein HuD disrupts postnatal cortical circuit maturation and behavior. *The Journal of neuroscience : the official journal of the Society for Neuroscience* **34**, 3674 (Mar 5, 2014).
58. A. A. Raposo *et al.*, Ascl1 Coordinately Regulates Gene Expression and the Chromatin Landscape during Neurogenesis. *Cell reports*, (Mar 4, 2015).
59. A. Ratti *et al.*, A role for the ELAV RNA-binding proteins in neural stem cells: stabilization of Msi1 mRNA. *Journal of cell science* **119**, 1442 (Apr 1, 2006).
60. S. Chung, M. Eckrich, N. Perrone-Bizzozero, D. T. Kohn, H. Furneaux, The Elav-like proteins bind to a conserved regulatory element in the 3'-untranslated region of GAP-43 mRNA. *The Journal of biological chemistry* **272**, 6593 (Mar 7, 1997).
61. G. E. Aranda-Abreu, L. Behar, S. Chung, H. Furneaux, I. Ginzburg, Embryonic lethal abnormal vision-like RNA-binding proteins regulate neurite outgrowth and tau expression in PC12 cells. *The Journal of neuroscience : the official journal of the Society for Neuroscience* **19**, 6907 (Aug 15, 1999).
62. A. Kozomara, S. Griffiths-Jones, miRBase: annotating high confidence microRNAs using deep sequencing data. *Nucleic acids research* **42**, D68 (Jan, 2014).
63. M. Y. Shah, G. A. Calin, MicroRNAs as therapeutic targets in human cancers. *Wiley interdisciplinary reviews. RNA* **5**, 537 (Jul-Aug, 2014).
64. D. De Pietri Tonelli *et al.*, miRNAs are essential for survival and differentiation of newborn neurons but not for expansion of neural progenitors during early neurogenesis in the mouse embryonic neocortex. *Development* **135**, 3911 (Dec, 2008).
65. D. Damiani *et al.*, Dicer inactivation leads to progressive functional and structural degeneration of the mouse retina. *J Neurosci* **28**, 4878 (May 7, 2008).
66. T. H. Davis *et al.*, Conditional loss of Dicer disrupts cellular and tissue morphogenesis in the cortex and hippocampus. *J Neurosci* **28**, 4322 (Apr 23, 2008).
67. K. Y. Kim *et al.*, A phosphomimetic mutant TDP-43 (S409/410E) induces Drosha instability and cytotoxicity in Neuro 2A cells. *Biochemical and biophysical research communications* **464**, 236 (Aug 14, 2015).
68. M. Ballarino *et al.*, TAF15 is important for cellular proliferation and regulates the expression of a subset of cell cycle genes through miRNAs. *Oncogene* **32**, 4646 (Sep 26, 2013).
69. S. Porta, L. K. Kwong, J. Q. Trojanowski, V. M. Lee, Drosha inclusions are new components of dipeptide-repeat protein aggregates in FTLTDP and ALS C9orf72 expansion cases. *Journal of neuropathology and experimental neurology* **74**, 380 (Apr, 2015).
70. S. Marcuzzo *et al.*, Altered miRNA expression is associated with neuronal fate in G93A-SOD1 ependymal stem progenitor cells. *Experimental neurology* **253**, 91 (Mar, 2014).
71. S. Marcuzzo *et al.*, Up-regulation of neural and cell cycle-related microRNAs in brain of amyotrophic lateral sclerosis mice at late disease stage. *Molecular brain* **8**, 5 (2015).
72. K. Nolan *et al.*, Increased expression of microRNA-29a in ALS mice: functional analysis of its inhibition. *Journal of molecular neuroscience : MN* **53**, 231 (Jun, 2014).

73. O. Butovsky *et al.*, Modulating inflammatory monocytes with a unique microRNA gene signature ameliorates murine ALS. *The Journal of clinical investigation* **122**, 3063 (Sep, 2012).
74. B. De Felice *et al.*, A miRNA signature in leukocytes from sporadic amyotrophic lateral sclerosis. *Gene* **508**, 35 (Oct 15, 2012).
75. D. Campos-Melo, C. A. Droppelmann, Z. He, K. Volkening, M. J. Strong, Altered microRNA expression profile in Amyotrophic Lateral Sclerosis: a role in the regulation of NFL mRNA levels. *Molecular brain* **6**, 26 (May 24, 2013).
76. N. Ludwig *et al.*, Distribution of miRNA expression across human tissues. *Nucleic acids research* **44**, 3865 (May 5, 2016).
77. S. Zongaro *et al.*, The 3' UTR of FMR1 mRNA is a target of miR-101, miR-129-5p and miR-221: implications for the molecular pathology of FXTAS at the synapse. *Human molecular genetics* **22**, 1971 (May 15, 2013).
78. M. J. Fogarty, E. W. H. Mu, N. A. Lavidis, P. G. Noakes, M. C. Bellingham, Motor Areas Show Altered Dendritic Structure in an Amyotrophic Lateral Sclerosis Mouse Model. *Frontiers in neuroscience* **11**, 609 (2017).
79. J. Weis *et al.*, Small-fiber neuropathy in patients with ALS. *Neurology* **76**, 2024 (Jun 07, 2011).
80. E. Dalla Bella *et al.*, Amyotrophic lateral sclerosis causes small fiber pathology. *European journal of neurology* **23**, 416 (Feb, 2016).
81. T. Tebaldi *et al.*, HuD Is a Neural Translation Enhancer Acting on mTORC1-Responsive Genes and Counteracted by the Y3 Small Non-coding RNA. *Molecular cell* **71**, 256 (Jul 19, 2018).
82. M. Amadio *et al.*, nELAV proteins alteration in Alzheimer's disease brain: a novel putative target for amyloid-beta reverberating on AbetaPP processing. *Journal of Alzheimer's disease : JAD* **16**, 409 (2009).
83. A. L. DeStefano *et al.*, Replication of association between ELAVL4 and Parkinson disease: the GenePD study. *Human genetics* **124**, 95 (Aug, 2008).
84. K. Haugarvoll *et al.*, ELAVL4, PARK10, and the Celts. *Movement disorders : official journal of the Movement Disorder Society* **22**, 585 (Mar 15, 2007).
85. M. A. Nouredine *et al.*, Association between the neuron-specific RNA-binding protein ELAVL4 and Parkinson disease. *Human genetics* **117**, 27 (Jun, 2005).
86. B. Akten *et al.*, Interaction of survival of motor neuron (SMN) and HuD proteins with mRNA cp15 rescues motor neuron axonal deficits. *Proceedings of the National Academy of Sciences of the United States of America* **108**, 10337 (Jun 21, 2011).
87. C. Fallini *et al.*, The survival of motor neuron (SMN) protein interacts with the mRNA-binding protein HuD and regulates localization of poly(A) mRNA in primary motor neuron axons. *The Journal of neuroscience : the official journal of the Society for Neuroscience* **31**, 3914 (Mar 9, 2011).
88. L. Hubers *et al.*, HuD interacts with survival motor neuron protein and can rescue spinal muscular atrophy-like neuronal defects. *Human molecular genetics* **20**, 553 (Feb 1, 2011).
89. Hao le T, Duy PQ, An M, et al. HuD and the Survival Motor Neuron Protein Interact in Motoneurons and Are Essential for Motoneuron Development, Function, and mRNA Regulation. *J Neurosci.* **37**, 11559 (Nov 29, 2017).
90. C. Fallini, G. J. Bassell, W. Rossoll, The ALS disease protein TDP-43 is actively transported in motor neuron axons and regulates axon outgrowth. *Human molecular genetics* **21**, 3703 (Aug 15, 2012).
91. De Santis, R., Alfano, V., de Turreis, V., Colantoni, A., Santini, L., Garone, M.G., Antonacci, G., Peruzzi, G., Sudria-Lopez, E., Wyler, E., et al. (2019). Mutant FUS and ELAVL4 (HuD) Aberrant Crosstalk in Amyotrophic Lateral Sclerosis. *Cell reports* **27**, 3818 (Jun, 25, 2019).
92. K. D. Anderson, M. A. Merhege, M. Morin, F. Bolognani, N. I. Perrone-Bizzozero, Increased expression and localization of the RNA-binding protein HuD and GAP-43 mRNA to cytoplasmic granules in DRG neurons during nerve regeneration. *Experimental neurology* **183**, 100 (Sep, 2003).
93. Strickland, E.R., Hook, M.A., Balaraman, S., Huie, J.R., Grau, J.W., and Miranda, R.C. MicroRNA dysregulation following spinal cord contusion: implications for neural plasticity and repair. *Neuroscience* **186**, 146 (Jun 14, 2011)
94. M. J. A. Wood, K. Talbot, M. Bowerman, Spinal muscular atrophy: antisense oligonucleotide therapy opens the door to an integrated therapeutic landscape. *Human molecular genetics* **26**, R151 (Oct 1, 2017).
95. K. M. Schoch, T. M. Miller, Antisense Oligonucleotides: Translation from Mouse Models to Human Neurodegenerative Diseases. *Neuron* **94**, 1056 (Jun 21, 2017).

96. Koval, E.D., Shaner, C., Zhang, P., du Maine, X., Fischer, K., Tay, J., Chau, B.N., Wu, G.F., and Miller, T.M. (2013). Method for widespread microRNA-155 inhibition prolongs survival in ALS-model mice. *Human molecular genetics* 22, 4127-4135
97. Butovsky, O., Jedrychowski, M.P., Cialic, R., Krasemann, S., Murugaiyan, G., Fanek, Z., Greco, D.J., Wu, P.M., Doykan, C.E., Kiner, O., et al. (2015). Targeting miR-155 restores abnormal microglia and attenuates disease in SOD1 mice. *Annals of neurology* 77, 75-99.

Journal Pre-proof

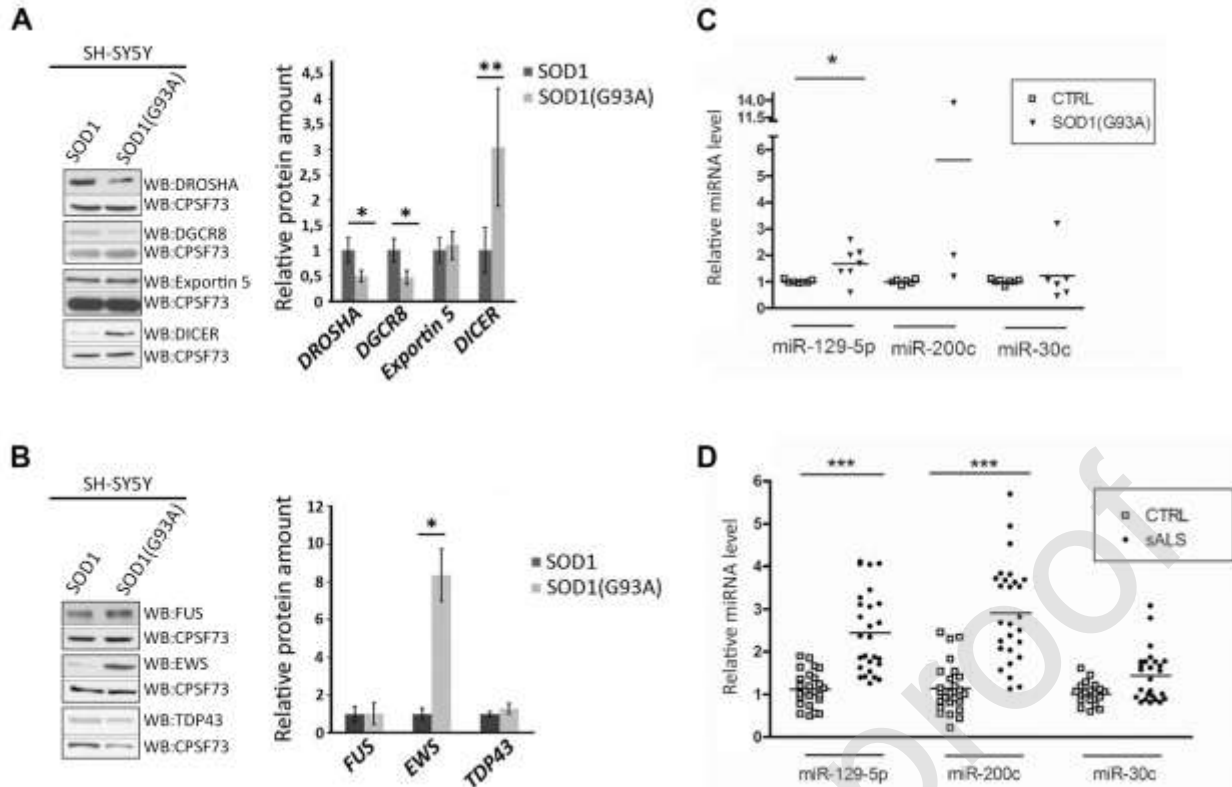


Figure 1. **Dysregulation of miRNA biogenesis in ALS.**

Dysregulation of miRNA biogenesis factors in SH-SY5Y/SOD1(G93A) cells.

A. *Left panel:* Representative Western blot analysis of components of the microprocessor complex. *Right panel:* Densitometric quantifications of the levels of the indicated proteins in SH-SY5Y/SOD1(G93A) cells compared to SH-SY5Y/SOD1 cells. Equal amounts of total protein extracts were fractionated on SDS-PAGE. Error bars represent the fold change standard deviation derived from at least three independent experiments (in particular: DROSHA n = 3; DGCR8 n = 7; DICER n = 7; Exportin 5 n = 4). Statistical significance between SOD1(WT) and SOD1(G93A) SH-SY5Y cells was determined by paired Student's *t*-tests; (**p* < 0.05; ***p* < 0.01).

B. *Left panel:* Representative Western blot analysis of DROSHA-interacting proteins. *Right panel:* Densitometric quantifications as in (A) of three independent experiments.

miR-129-5p is upregulated in SOD1(G93A) transgenic mice and in PBMCs of sALS patients.

C. RT-qPCR analysis of miRNA expression in transgenic SOD1(G93A) mice. Total RNA was extracted from the spinal cord of seven mice at the early stage of disease (15 weeks) and of seven age-matched non-transgenic control mice. Relative levels of miR-129-5p, miR-200c and miR-30c were determined; RNU1A1 was used as an internal control for normalization. Data are presented as box plot graphs of three technical replicates for each measurement. Statistical significance was determined using unpaired Student's *t*-test, * denotes *p* < 0.05.

D. RT-qPCR analysis of miR-129-5p, miR-200c, and miR-30c levels in human PBMCs. The relative abundance of these three miRNAs was measured in PBMC-extracted RNA from 27 patients with sporadic

ALS and 25 control subjects. snoRD25 and miR-16 were used as internal controls for normalization. Statistical analysis as in C (***) $p \leq 0.001$).

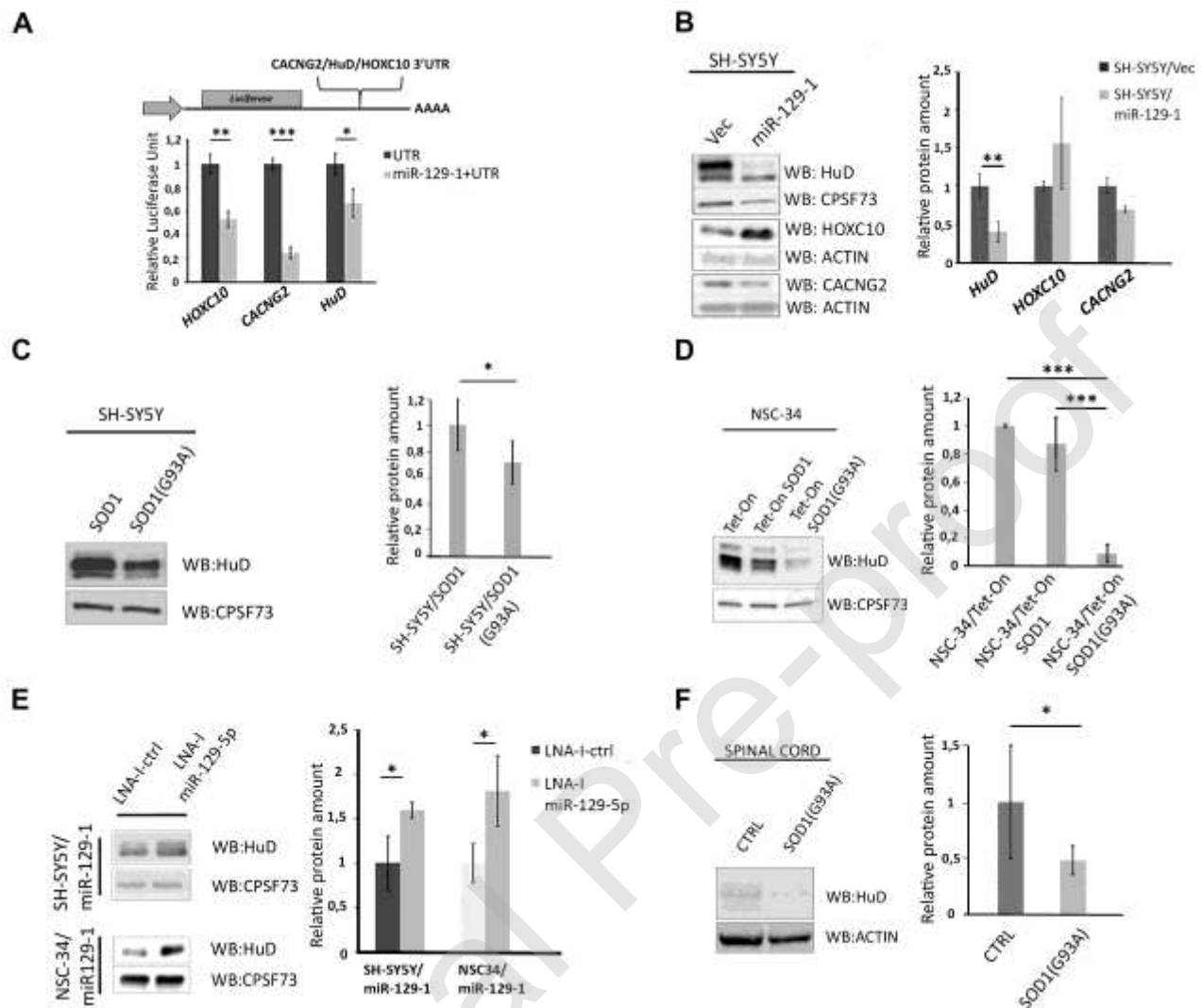


Figure 2. **HuD mRNA is a target of miR-129-5p.**

A. *Upper panel*: Schematic representation of the firefly luciferase reporter constructs depicting the insertion site of the indicated 3'UTR sequences. *Lower panel*: Relative firefly luciferase activity was determined in cells overexpressing miR-129-1 (gray bars) or not (black bars) and expressing firefly reporter constructs harboring the 3'UTRs of HOXC10, CACNG2 or HuD. A *Renilla* luciferase-expressing plasmid was used as an internal transfection control. For each firefly construct, the firefly luciferase activities were normalized to *Renilla* luciferase activity, and the values obtained without miR-129-1 overexpression were set as 1. The mean \pm s.e.m. of three independent experiments is shown. Statistical significance was determined as in Figure 1A.

B. Western blot analysis of the endogenous HuD, HOXC10 and CACNG2 proteins in human SH-SY5Y cells stably expressing the precursor miR-129-1. *Left panel*: representative Western blot. *Right panel*: Densitometric quantification. Error bars represent the fold change standard deviation derived from two

independent experiments (n = 3 for HuD). Statistical significance was determined as in Figure 1A; (**p < 0.01). CPSF73 and actin were used as loading controls.

HuD is downregulated in models of SOD1-linked ALS.

C. *Left panel*: representative Western blot of endogenous HuD protein from SH-SY5Y cells stably expressing either the wild type (WT) SOD1 protein or the ALS-associated SOD1(G93A) mutant. CPSF73 was used as loading control. *Right panel*: Quantification and statistical analysis of five independent experiments was determined as in Figure 1A; (* p < 0.05).

D. *Left panel*: representative Western blot of endogenous HuD protein from NSC-34 cells expressing either the wild type SOD1 protein or the SOD1(G93A) mutant under a doxycycline-inducible promoter. CPSF73 was used as loading control. *Right panel*: Quantification and statistical analysis of three independent experiments as in Figure 1A.

E. LNA miR-129-5p rescued HuD protein expression. *Left panel*: Western blot analysis of HuD protein levels in SH-SY5Y/miR-129-1 and NSC-34/miR-129-1 cells transiently transfected with a scrambled LNA control or a miR-129-5p inhibitor LNA oligonucleotide. CPSF73 was used as loading control. *Right panel*: Quantification and statistical analysis of three independent experiments as in Figure 1A.

F. *Left panel*: representative Western blot of endogenous HuD protein derived from spinal cord of wild type or SOD1(G93A) mutant mice. Actin was used as loading control. *Right panel*: Quantification and statistical analysis of six independent experiments was determined by unpaired Student's t-test; (*p < 0.05).

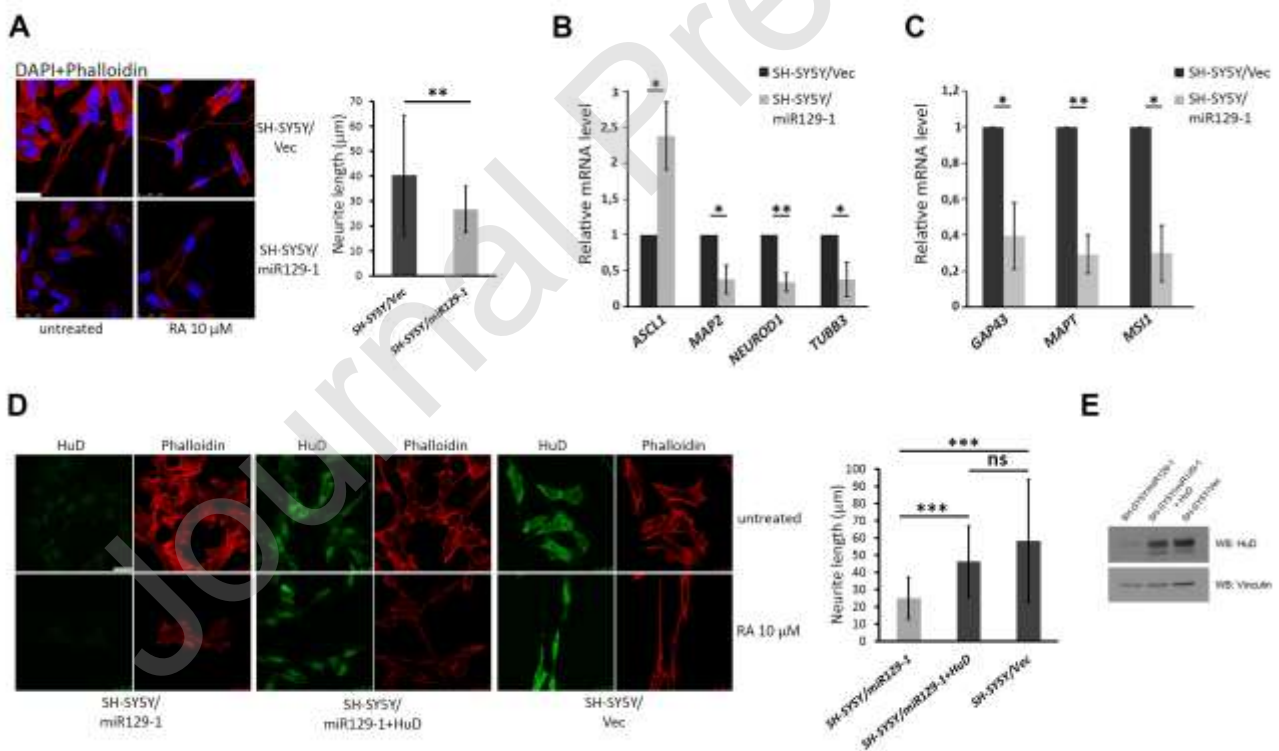


Figure 3. miR-129-5p overexpression inhibits neurite outgrowth and differentiation by downregulating HuD.

- A. *Left panel:* Magnification of representative confocal micrographs of control (Vec) and miR-129-5p-overexpressing (miR-129) SH-SY5Y cells. Neuronal differentiation was induced by treatment with 10 μ M retinoic acid (RA) for eight days, and neurites were visualized by phalloidin staining (red). Nuclei were stained with DAPI. Scale bars represent 25 μ m. *Right panel:* Neurites length quantification was performed by manually tracing the longest neurite per cell, as described in Supplementary Material and Methods. Average neurite length and standard deviations from three independent experiments are shown. Statistical significance was determined by unpaired Student's *t*-test, ** denotes $p < 0.01$.
- B. Expression of neuronal markers after RA-induced differentiation. Relative mRNA levels of ASCL1, MAP2, NEUROD1, and TUBB3 were measured by RT-qPCR in total RNA purified from SH-SY5Y and in SH-SY5Y/miR-129-1 cells after treatment with RA for eight days. LDH mRNA was used for normalization. Average values and standard deviations from three independent experiments are shown. Statistical significance was tested by unpaired Student's *t*-test, * denotes $p < 0.05$.
- C. Expression of HuD-targeted transcripts after RA-induced differentiation. Relative mRNA levels of GAP43, MAPT, and MS11 were measured by RT-qPCR as in (B). ** denotes $p < 0.01$.
- D. *Left panel:* Exogenous expression of miR-129-5p-insensitive HuD restores neuritogenesis in SH-SY5Y/miR-129-1 cells. Representative confocal micrographs are shown of undifferentiated (untreated) or differentiated (10 μ M RA for eight days) SH-SY5Y cells transfected either with the miR-129 either empty vector (Vec) or with a plasmid expressing the HuD open reading frame. Cells were stained with phalloidin (red) and anti-HuD antibody (green). Scale bars represent 25 μ m for magnified micrographs. *Right panel:* Quantification and Statistical significance was determined as in Figure 3A, *** denotes $p < 0.001$.
- E. Western blot analysis of HuD expression of the cell lines described in (D). Vinculin was used as a loading control.

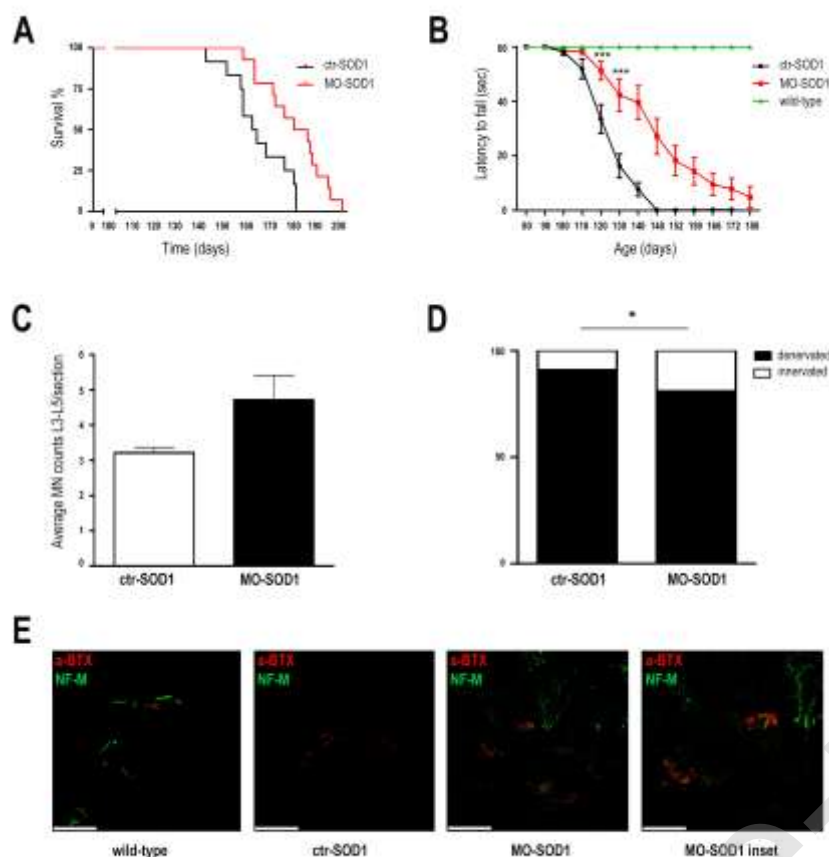


Figure 4 **MO-miR-129 ameliorates the pathological phenotype in the SOD1 (G93A) mouse model.**

A. Kaplan-Meier survival curves demonstrated a significantly extended median survival by 22 days in MO-SOD1 mice ($n = 14$) compared to ctr-SOD1 animals ($n = 12$) (median survival: MO-SOD1 mice 180 days, ctr-SOD1 mice 160 days; $\chi^2 = 7.232$, $p = 0.0072$, log-rank test).

B. Inverted grid curve data were significantly ameliorated in MO-SOD1-treated mice compared to ctr-SOD1-treated mice ($n = 12$ /group). Data are reported as the mean \pm SEM for each time point expressed in seconds. $***p < 0.001$, repeated measures ANOVA with Sidak's post-analysis. Data were analysed up to 130 days, when all animals in each group were still alive.

C. Quantification of MNs in the lumbar spinal cords (L3-L5) of MO-SOD1-treated mice and ctr-SOD1 mice (mean \pm SEM). A trend toward reduced MN loss in the treatment group was observed, although this change was not statistically significant; $n = 30$. Student's t-test, 4 mice/group, $p = 0.08$.

D. Quantification of the merged signal showed a significant increase in NMJ innervation tibial anterior (TA) muscles in MO-SOD1-treated mice ($n = 4$) compared to ctr-SOD1-treated mice ($n = 4$). $*p < 0.05$, contingency chi-squared test ($\chi^2 = 4.153$), $n = 100$ NMJs analysed for each animal.

E. Representative image of NMJ in TA muscles. Axons of presynaptic MNs were stained with antibody raised against neurofilament medium (NF-M) (green). The acetylcholine receptors of the postsynaptic termini were labelled with α bungarotoxin (α BTX; red). The overlay of both signals (yellow) indicates innervation at

the motor end-plate. In ctr-SOD1 mice, the presynaptic termini present a collapsed structure, suggesting a pathologic NMJ, while MO-SOD1 treatment ameliorates NMJ structure and innervation. Scale bar: 75um, inset: 50um

Journal Pre-proof

Table 1. Differentially expressed miRNAs in SH-SY5Y/SOD1(G93A) cells.

ENSEMBL ID	MiR	Log2 FC
ENSG0000199077	has-mir-129-2	3,30
ENSG0000207598	has-mir-124-3	-2,70
ENSG0000207705	has-mir-129-1	2,66
ENSG0000207703	has-mir-7-2	2,50
ENSG0000207713	has-mir-200c	2,14
ENSG0000221419	has-mir-1287	2,29
ENSG0000221630	has-mir-1179	2,44
ENSG0000216135	has-mir-885	-2,58
ENSG0000207726	has-mir-455	-1,74

Table 2. **Clinical and demographic data of the recruited subjects.**

ALSFERS-R, ALS functional rating scale-revised version; DPI, disease progression index; n.a., not applicable; NIV, non-invasive ventilation; PEG, percutaneous endoscopic gastrostomy; *50 mg bid.

	CTRL n=25	sALS n=27
Sex, M/F	12 / 13	12 / 15
Age, years	63.8 ± 11.7 (38-78)	62.7 ± 12.1 (41-78)
Duration, months	n.a.	29.8 ± 27.7 (0-102)
Onset, Bulbar/Spinal	n.a.	8 / 19
ALSFERS-R	n.a.	22.2 ± 7.3 (5-37)
DPI	n.a.	0.82 ± 0.51 (0.17- 1.77)
PEG, yes/no	n.a.	7 / 20
NIV, yes/no	n.a.	8 / 19
Riluzole, yes/no *	n.a.	26 / 1